Original Article

JOURNAL OF REINFORCED PLASTICS & COMPOSITES

Journal of Reinforced Plastics and Composites
2015, Vol. 34(6) 479–492

DOI: 10.1177/0731684415573981
jrp.sagepub.com
SAGE

Compression moulding of sheet moulding compound: Modelling with computational fluid dynamics and validation

NE Jimmy Kluge[1], T Staffan Lundström[1], Lars G Westerberg[1] and Kurt Olofsson[2]

Abstract
Compression moulding experiments of sheet moulding compound, visual observations of a vacuum test with prepregs and numerical models with two main approaches for computational fluid dynamics simulations of the mould filling phase are presented. One assumes that there are layers near the mould surfaces with much less viscosity and the other only use one viscosity model. The numerical experiments showed that the pressure could be accurately predicted with both approaches. The property necessary to predict correct pressure with altered mould closing velocities was that the bulk material had to obey shear-thinning effects. Preheating effects before compression were neglected, but altering the heating time until the prepreg was assumed to start flow had a significant effect. The experiments confirmed that the pressure is predominantly affected by the mould closing velocity. Regardless of the considered process settings, a first pressure top always appeared approximately at the logarithmic strain 0.25. A second top was associated with a slow-down of the press. The location of this was affected by the velocity and the vacuum, the latter indicating that vacuum assistance prevents a build-up of back pressure. Furthermore, heated prepreg above a critical temperature is observed to swell immediately as vacuum assistance is applied.

Keywords
Sheet moulding compound, computational fluid dynamics, modelling, compression moulding

Introduction

Compression moulding of sheet moulding compound (SMC) is a fast manufacturing method for fibre reinforced composite products. The process can be divided into two main steps: preparation and moulding of SMC prepreg. In the preparation step, prepreg sheets are manufactured that consist of a paste that impregnates more or less randomly distributed fibres that are spread and impregnated in the plane of the sheets. Fibre orientation has interestingly moderate effect on the global stiffness, for example a hood as shown by Oldenbo et al.[1] The composition of the ingredients building these prepregs can be made in uncountable ways to give the prepregs special rheological characteristics during manufacturing or to give the finalized product fire retardant properties, for instance. In general, however, the prepregs mainly consist of a thermosetting polyester resin, calcium carbonate fillers and glass fibre reinforcements. In the moulding process, charges of stacked prepreg sheets are placed inside a heated moulding tool and as the mould closes, the charge is forced to flow and fill the cavity of the moulding tool. The mould is then kept closed until the thermosetting resin has cured. With this method quite advanced shapes can be manufactured, and due to the usage of prepregs the manufacturing process is rather fast and

[1]Division of Fluid and Experimental Mechanics, Luleå University of Technology, Luleå, Sweden
[2]Swedish Institute of Composites, Swerea SICOMP AB, Piteå, Sweden

Partly presented in Interdisciplinary Transport Phenomena VII, Dresden, Germany, 19–23 September 2011.

Corresponding author:
NE Jimmy Kluge, Division of Fluid and Experimental Mechanics, Luleå University of Technology, SE-971 87 Luleå, Sweden.
Email: jimmy.olsson@ltu.se

therefore suitable for large scale productions, e.g. lightweight composite products in the vehicle industry where it is of great importance to achieve a high quality of the surface appearance. This property is an issue for SMC manufacturers since voids located at the surface level sometimes cause so called pinholes or blowouts, see Sjögren.[2] Voids inside the material is also of concern for the high voltage industry since voids decreases the electrical insulation properties.[3,4] Air entrapments during paste mixing and poor bundle impregnation not only have been observed as two sources to voids, but also that these voids are removed during compression moulding by Comte et al.[5] One possible reason for the voids is that air is entrapped during the preparation of the prepregs or that the entrapped air that has dissolved into the resin nucleate in low pressure zones during the compression stage as suggested by Lundström and Holmgren.[6] It is furthermore also possible that air entrapments can form due to complex flow at the flow front during compression as described by Odenberger et al.,[7] where a squish effect was observed when the flow front was experimentally visualised during compression moulding. At the end of the flowing stage, boiling of styrene was observed as well,[7] which also can result in voids in the final part. Several processing parameters have been found to reduce the amount of voids during compression moulding. For example, increased mould closing pressure, preheating of the SMC charge,[8] vacuum assisted moulding,[4,9] and increased mould closing velocity.[4] A common effect of these measures, except mould pressure, is that they seem to cause a more homogenous flow.[4,7,10] Olsson et al.,[4] used multi coloured SMC sheets to study the effects from velocity, temperature, and vacuum assistance on the final flow pattern of moulded SMC plates. It was observed that at high mould closing velocity ($10\,\mathrm{mm\,s^{-1}}$), the flow become homogenous without the assistance of vacuum, but by applying vacuum assistance and using the lower mould temperature (420 K vs. 430 K), it also became homogenous at the low closing velocity ($2.5\,\mathrm{mm\,s^{-1}}$). Hence, to be able to reduce the void content in finished SMC parts it is crucial to develop models that accurately can predict the flow of SMC and from those models develop moulding tools, charge patterns, and prepreg materials in order to avoid flows that are more likely to cause voids. In addition to higher quality of manufactured products, money could be saved since development of moulding tools and charge lay-ups for new products is often preceded by some testing before the manufacturing comes to full capacity. The complexity of the prepreg material aggravates rheological measurements that might facilitate the development of models for computational simulation. Many have though made prominent work on the rheology of SMC.

Rheology of SMC

It has been shown that the paste used to create SMC prepregs, itself without added fibres, behaves as a non-Newtonian fluid with shear thinning properties.[11,12] Nevertheless the viscosity of the paste as a function of temperature has been described as

$$\eta_{paste} = \eta_0 e^{-b\left(\frac{1}{T_0}-\frac{1}{T}\right)} \tag{1}$$

by Le Corre et al.,[12] where T is temperature, b is a temperature constant, and the subscript 0 denotes initial conditions. Equation (1) is often combined with an expression stating that the shear viscosity is a power law function of the shear rate implying a non-Newtonian behaviour. It have also been observed that the viscosity of the paste can be described by a Carreau viscosity model by Lee et al.[11] If the viscosity is assumed to be very small at infinitive shear, the Carreau viscosity model reduces to

$$\eta = \eta_{zs}\left(1+(\lambda\dot{\gamma})^2\right)^{\frac{n-1}{2}} \tag{2}$$

where $\eta_{zs} = \eta_{zs}(T)$ is the zero shear rate viscosity, λ is the time constant, $\dot{\gamma}$ is the shear strain rate, and n is the power law constant. This means that the paste behaves as a Newtonian fluid at low shear rates, and as the temperature increases, the Newtonian transition area moves to higher shear rates. It is widely accepted that unreinforced polymers and melts usually have a shear-dominated mould flow and that their flow behaviour can be modelled without considering the extensional viscosity dissipation.[13] However, when modelling materials such as SMC with planar fibre suspensions, it is popular to assume a gap-wise velocity profile that is close to a plug flow and that the main viscosity dissipation being in-plane extension since many experiments have shown that SMC deform in a biaxial extensional flow mode with very little mixing between the prepreg layers and extensive slip along the mould walls.[14] It has also been shown that shearing effects can be significant even though the biaxial extension indeed dominates in most cases of fibre suspension squeeze flows.[13] When fibres are added into the plane of sheets, the compression viscosity, or elongation viscosity, is much more affected than the shear viscosity. The compression viscosity of SMC with fibres has been found to be a function of the paste viscosity, η_{Paste}, and the volume fraction of fibres, f_f, added to the paste according to the expression below by Le Corre et al.[12]

$$\eta_{Compression} = 3\cdot\eta_{Paste}(T)\cdot\left(\frac{\dot{\varepsilon}}{\dot{\varepsilon}_0}\right)^{n-1}\cdot\left(1+\beta\frac{f_f}{1-f_f}\right) \tag{3}$$

Here β is a constant (=360 in Le Corre et al.[12]) being independent of the temperature and $\dot{\varepsilon}$ is the strain rate ($\dot{h}/h$). Later, in a subsequent study by Dumont et al.,[15] it was found that a quadratic relationship is more suitable. Hence, by revising equation (3) into

$$\eta_{Compression} = 3 \cdot \eta_{Paste}(T) \cdot \left(\frac{\dot{\varepsilon}}{\dot{\varepsilon}_0}\right)^{n-1} \cdot \left(1 + 100 \cdot f_f + 1000 \cdot f_f^2\right) \quad (4)$$

a better fit to experiments is obtained by Le Corre et al.,[12] especially at low strain rates. It is in the context worth mentioning that the effect of fibres on the shear viscosity is not that dramatic; it has for example been observed by Le Corre et al.[12] that by adding about 11 volume percentage of fibres, the shear viscosity is only increased by a factor of 3. Finally Le Corre et al.[12] derived a compression viscosity as

$$\eta_{Compression} = \frac{\sigma_{Threshold}}{\dot{\varepsilon}} \quad (5)$$

and it was found that the result followed a power law relationship with $n = 0.3$. With a multiobjective surrogate-based inverse modelling technique, Marjavaara et al.[16] managed to obtain simulations capturing the flow behaviour of SMC with usage of the following formula:

$$\mu(T) = Ae^{-b(T-T_0)} \quad (6)$$

Also, the pressure could successfully be predicted but unfortunately not at two locations simultaneously. Hence, the main goal for this study is to extend equation (6) to an expression that adequately predicts the pressure at several locations at the same time.

As previously mentioned, it is popular to assume a gap-wise velocity profile that is close to a plug flow when modelling the flow of SMC. In reality, it is, however, observed in several experimental studies that the flow might be much more complex. The flow front of SMC during compression has for example been visualised by Odenberger et al.[7] It was observed that the flow was initiated by an initial squish effect where the SMC prepreg closest to the mould surfaces shoot away strongly before the inner layers even started to move. At the end when the mould had closed, boiling could be seen at the surface of the flow front. This was addressed as boiling styrene. It might be speculated that the observed boiling also could be enclosed air that left the material due to the high pressure.

The behaviour with less flow for the inner layers was also observed by Olsson et al.[4] where coloured SMC was used to visualize the final flow pattern of SMC in an factorial process parameter experiment where the tested factors in the experiment were vacuum assistance, mould closing velocity, and temperature of the moulding tool. The results showed that all of these factors had an influence on the global flow behaviour. High (10 mm s^{-1}) mould closing velocity tends to create a more uniform flow. It was moreover also observed that a more uniform flow could be achieved by utilizing vacuum assistance when the mould closing velocity was slow (2.5 mm s^{-1}). By increasing the mould temperature, the inner layers were allowed to stretch further, but this also increased the squish effect from the outer layers. In the same work an additional experimental run was made where the quality of moulded plates (not coloured) was quantified by multiple high voltage insulation tests. The ability to resist a disruptive discharge was interpreted as a measure of the relative amount of voids in the moulded samples since voids are known to decrease the electrical insulation properties.[3] A main effect was that the outer area of the plates where the SMC had flown the furthest had a higher ability to withstand electrical discharge. The amount of voids was ergo interpreted to be smaller in this area. Interestingly, it was also observed that the parameter settings that resulted in more uniform flows in the coloured SMC experiment, high mould closing velocity, or applied vacuum assistance at low mould closing velocity, also improved the electrical insulation properties and hence reduced the amount of voids, according to the assumption made about relationship between voids and electrical insulation.

An indication of the complex flow of SMC has also been disclosed with X-ray phase contrast microtomography by Le et al.[8] Before moulding it was observed that the plies themselves consisted of a core zone with a high amount of fibres between an upper and lower skin which consisted of a small amount of fibres.[8] When the charges were moulded, the skins with less fibres had disappeared for the plies placed inside the charge. However, the skins remained at the upper and lower plies that were in contact with the mould wall. The thickness of respective skin remained approximately constant, 0.26 mm for the bottom layer, and 0.22 mm for the upper layer, independent of process settings, placement of charge, and preheat temperature of the charge. This result implies that the SMC is highly sheared at the mould walls due to a low viscosity of a compound without fibres and it was suggested that plug flow models probably can be applied to describe the flow of the core zone.[8] It have however been observed by Rabinovich et al.[17] that the amount of glass fibres have an effect on the thickness of the lubricating layer.

Experimental set-up

An experimental moulding tool of circular geometry with two pressure sensors and with vacuum assistance

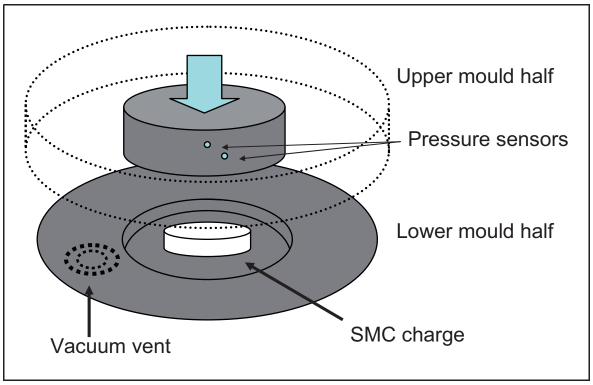

Figure 1. Schematic illustration of the experimental setup. The radii of the SMC charge and the mould cavity are 75 mm and 159 mm, respectively. As the upper mould half goes down it encapsulates the cavity which enables the use of vacuum assistance.

Table 1. Composition of the paste.[a]

Resin	Mass %
Resin	19.3
Low-profile additives	8.9
Fillers	66.8
Inhibitor	2
MgO	0.77
Internal release agents	1.5
Wetting agent	0.46

[a]In addition fibres were added to an amount that took up a weight of 26–27% of the total weight of the paste and fibres.

capability was used for the experiments; see Figure 1 for details. The moulding tool itself was mounted in a Fjellman press that was programmed to run at different velocities and temperatures. During this study, a standard industrial low-profile prepreg was used as experimental material; see Table 1 for a summary of the material composition.

From the prepreg, circular sheets of a diameter of 0.15 m were prepared. The sheets were thereafter stored in air sealed vessels in order to avoid significant styrene loss before they were randomly picked for the experiments where they were put into stacks each built-up by seven layers. This procedure resulted in an average height of 14.7 mm of the stacks. The weight of each stack was controlled before it was placed in the centre of the moulding tool. During the experiments the charges were placed by hand inside the mould. To increase repeatability and shorten the time that the charge had to reside inside the hot moulding tool before it was moulded, markings were

Table 2. Process settings in the two-level factorial design experiment.

Level	Low (−1)	High (1)
Vacuum	0%	75%
Velocity	2.5 (mm s^{-1})	10 (mm s^{-1})
Temperature	420 (K)	430 (K)
Pressure	450 (kN)	450 (kN)

made inside the tool, enabling a fast and accurate manual loading of the charges. Thereafter the press was manually started, a process approximated to 5 s. The press was programmed to run with very high velocity down to the height 40 mm where it slowed down and finally reached the desired constant velocity of 2.5 or 10 mm s^{-1}. Due to the different velocities, it took an additional 12.7 s for the slow velocity until the upper mould surface reached the charge and 3.6 s for the fast velocity.

Pressure data from compression mouldings were obtained from process parameter experiments where the altered parameters were vacuum level inside the mould, mould closing speed, and the temperature of the moulding tool. The experiments were performed as a two-level factorial design experiment with split plot design methodology since it was very time consuming to alter the temperature of the moulding tool; see Table 2 for the process settings. Each setting was replicated four times, giving a total of 32 samples. The commercial software MiniTab 16 was used to facilitate planning and analysis of the experiments.

Results that will be shown later in the experimental result section indicated that something happened to the prepreg while vacuum assistance was applied. Therefore an additional experiment was organised where visual observations of prepreg at 25°C, 50°C, and 80°C inside a transparent vessel were performed while vacuum was applied.

Numerics

In this work, simulations of the mould closing and resultant SMC prepreg flow have been performed with several viscosity models for the SMC prepreg material. This was done in order to evaluate if any of the models could predict the pressure accurately during the compression phase. All of the models that will be presented later have in common that they consist, inter alia, of two unknown constants, A and B, representing the prepreg viscosity without any shear-thinning effect and its sensitivity to alternations in temperature, respectively. The method chosen to find the proper values of these constants has been to use combined response surfaces, each built with a design of experiment (DOE) approach. Ansys Workbench and CFX were used to create the response surfaces and simulations, respectively. Combined response surfaces implies that two response surfaces for the pressure are built for each model, one at the beginning when the stacks have been compressed 1 mm, and one near the end of the moulding when the compression distance had increased to 6 mm. This was done for the slow closing velocity. Initially, very broad ranges of the constants were chosen in order increase the chance of finding proper values within the ranges. The matching of equation (1) to the data in Lee et al.[11] result in $B = 11{,}700$, which is significantly higher than reported in Le Corre et al.[12] and Dumont et al.[18] where $B = 4900$ and 4500, respectively. Following these results constrictions were set to $2000 < B < 12{,}000$ while $200{,}000 < A < 1.7 \times 10^6$. The latter restrictions were estimated by altering η_0 in the Equation below.

$$A = \eta_0 3\left(1 + 100 f_f + 1000 f_f^2\right) \tag{7}$$

Equation (7) originates from Dumont et al.[15] where f_f was set to 0.2 for the conditions presented here. From each of these response surfaces, many combinations of the unknown constants can be found that give the desired pressure that was found in the real experiment. However, combining these possible combinations from both response surfaces in one plot, with A and B on the axes, reveals fortunately that there is only one particular combination of the two constants that result in the desired pressure both at the beginning and the end of the moulding, see Figure 2.

The obtained values were then used in a new simulation in order to verify the settings. Interestingly, all models yielded that the setting decided by the intersection of the two curves did not produce the correct pressure curve. This was due to the fact that very broad ranges were initially allowed for the constants A and B since little was known about their real values. As a consequence, the first response surfaces failed in representing the real response. Therefore, new values of the constants and the results from the verifying simulation were manually added as a refinement points in both response surfaces. Hence, the response surfaces could step by step be improved in the area where it was likely that the proper values of A and B could be found. This was repeated until neither the standard second order polynomial nor the neural network could give a better response surface. For some models, a response surface of the Kriging type had to be used in the last step to predict the constants A and B. This approach was applied since these are forced to pass through the

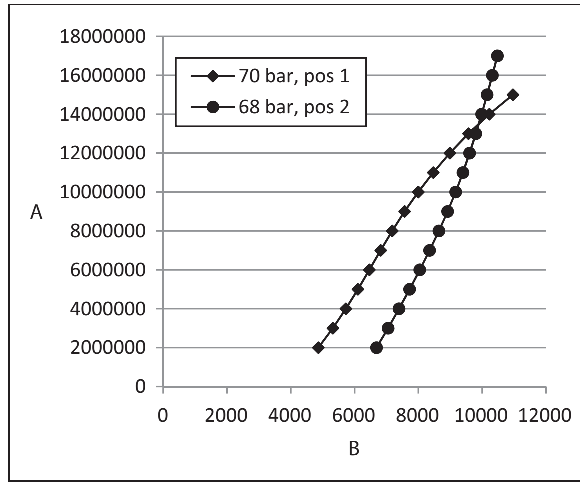

Figure 2. Example of how results from two response surfaces were used together to find one combination of the constants A and B that gave the desired pressure both in the beginning and end of the moulding. The markers are constant combinations that were manually picked from the response surfaces that gave the desired pressure.

design points. The response surface in the area of interest, which at this instant had several refinement points, was hence not as affected by design points far away. When constants for the different models were found that gave desired pressure for the slow mould closing velocity, the same constants were also inserted into simulations with the higher mould closing velocity in a further trial to investigate if the model also could predict the pressure at changed conditions. The simulations with higher mould closing velocity also got their initial preheating time adjusted to 0.35 s since their contact with upper and lower mould tool before the SMC stack is assumed to flow is shorter.

Geometry and mesh

In the experiments it could be seen that the pressure top occurred approximately at the same height regardless of processing parameters used. The same behaviour has previously been observed in Le Corre et al.,[12] where it was concluded that the pressure seemed to reach a maximum at the logarithmic strain, $\varepsilon = 0.25$ ($\varepsilon = \ln(h_0/h)$). By observing the SMC charge, it was concluded that the flow was not initiated until after the pressure top.[12] This delay in motion was addressed to air removal. Hence, it is likely that the SMC charge is only compressed until the first pressure top. Therefore, the virtual model is setup to start at 11.4 mm which was the average height at where the pressure top occurred. This condition is interestingly also the logarithmic strain $\varepsilon = 0.25$. The cylindrical geometry of the experimental moulding tool is also applied in the numerical model.

Since the geometry is axisymmetric, it can be modelled as a slice with symmetry boundary conditions. The slice is made up of one layer that is extruded 1°. The initial mesh can be seen in Figure 3. Each time step, this mesh then deformed to simulate that the mould closed. Deformations were chosen to appear far away from boundaries and the final mesh can be seen in Figure 4.

Heat transfer

Thermal conductivity experiments by Olofsson and Sandlund[19] performed on a similar prepreg as the one used in the experiments yielded a value of 0.78 W m^{-1} K^{-1} during heating up to 80°C. Later, during cooling from 120°C to room temperature, the value of 0.98 W m^{-1} K^{1} was found. The increase was traced to decreased levels of air inside the stack after curing. Therefore, the value 0.78 W m^{-1} K^{-1} will here be used to reflect the initial conditions in the stack while later during compression the value 0.98 W m^{-1} K^{-1} is applied when much of the air is removed. When calculating these values, the density of the prepreg was measured to 1.816 g cm^{-3} and the value 1300 J kg^{-1}°C^{-1} was used as specific heat capacity. These data will be applied here as well but, since the stack is assumed to be compressed before the flow is initiated, the density is adjusted to 2330 kg m^{-3}. A common assumption when modelling compression moulding of SMC is that the heat transfer to the prepreg prior to compression can be neglected. This is done here as well, but the heat transfer from the tool to the prepreg during the time from when the upper mould half reaches the prepreg

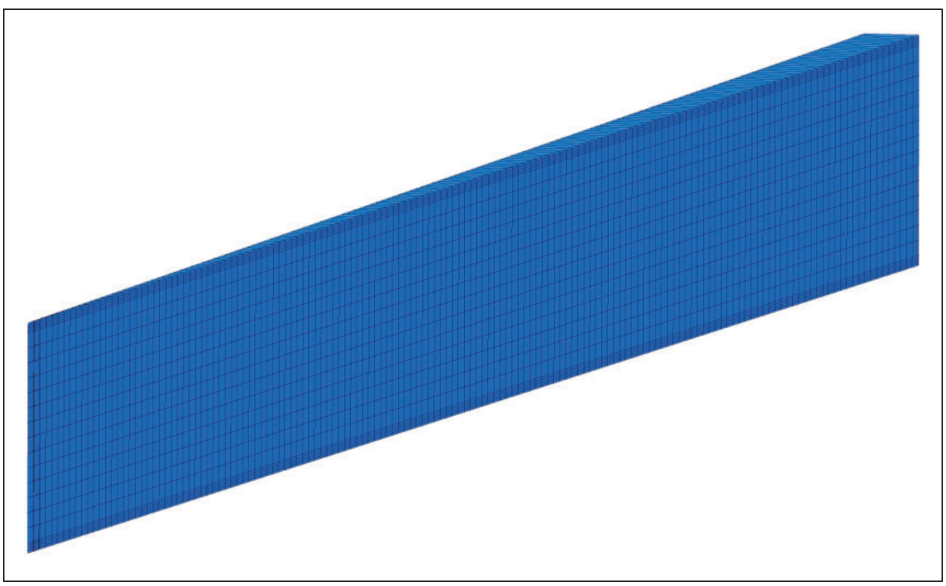

Figure 3. The initial mesh in the first time step.

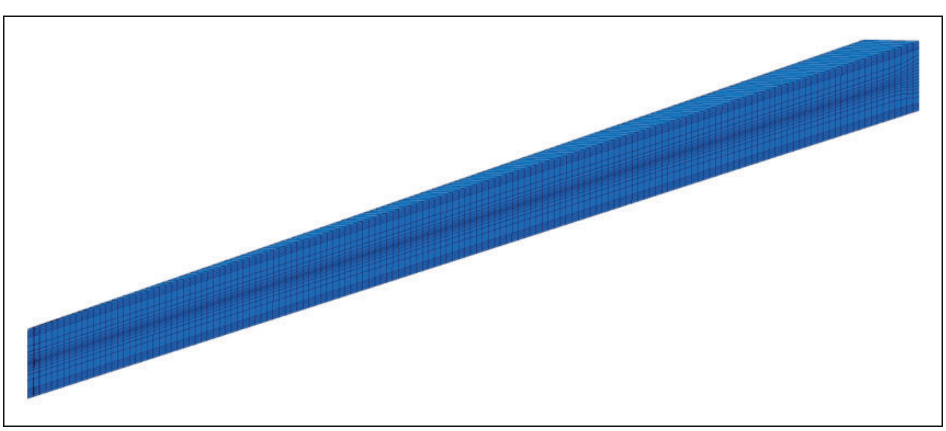

Figure 4. The deformed mesh in the last time step.

Table 3. Description of the different numerical models used in this work.

Models		Skin viscosity	Bulk viscosity
1	Only bulk, shear thinning.	-	$Ae^{-B\left(\frac{1}{T_0}-\frac{1}{T}\right)}\left(\frac{\dot{\varepsilon}}{\dot{\varepsilon}_0}\right)^{n-1}(1+\dot{\gamma}^2)^{\left(\frac{n-1}{2}\right)}$
2	Only bulk, shear thinning with a Newtonian plateau.	-	$Ae^{-B\left(\frac{1}{T_0}-\frac{1}{T}\right)}\left(\frac{\dot{\varepsilon}}{\dot{\varepsilon}_0}\right)^{n-1}(1+\lambda\dot{\gamma}^2)^{\left(\frac{n-1}{2}\right)}$
3	Bulk and skins, both shear thinning.	$A\frac{3}{61}e^{-B\left(\frac{1}{T_0}-\frac{1}{T}\right)}(1+\dot{\gamma}^2)^{\left(\frac{n-1}{2}\right)}$	$Ae^{-B\left(\frac{1}{T_0}-\frac{1}{T}\right)}\left(\frac{\dot{\varepsilon}}{\dot{\varepsilon}_0}\right)^{n-1}(1+\dot{\gamma}^2)^{\left(\frac{n-1}{2}\right)}$
4	Bulk and skins, both shear thinning with a Newtonian plateau	$A\frac{3}{61}e^{-B\left(\frac{1}{T_0}-\frac{1}{T}\right)}(1+\lambda\dot{\gamma}^2)^{\left(\frac{n-1}{2}\right)}$	$Ae^{-B\left(\frac{1}{T_0}-\frac{1}{T}\right)}\left(\frac{\dot{\varepsilon}}{\dot{\varepsilon}_0}\right)^{n-1}(1+\lambda\dot{\gamma}^2)^{\left(\frac{n-1}{2}\right)}$
5	Bulk and skins, only shear thinning in skins.	$A\frac{3}{61}e^{-B\left(\frac{1}{T_0}-\frac{1}{T}\right)}(1+\dot{\gamma}^2)^{\left(\frac{n-1}{2}\right)}$	$Ae^{-B\left(\frac{1}{T_0}-\frac{1}{T}\right)}\left(\frac{\dot{\varepsilon}}{\dot{\varepsilon}_0}\right)^{n-1}$

until the prepreg is assumed to start flow at $\varepsilon = 0.25$ is accounted for since it is assumed that the contact between the surfaces is good in this case. Therefore, the preheating time for the upper and lower side of the SMC were arbitrary set to 0.35 s for the simulations at 10 mm s^{-1} and 1.3 s for simulations at 2.5 mm s^{-1}.

The viscosity models

As previously stated it has been observed that moulded SMC obtains skins near the mould tool surface with less amounts of fibres than the bulk material. It is believed that the material is highly sheared in these zones on the contrary to the bulk flow were it is believed to be dominated by elongational flow. In previous simulation work with SMC, the SMC prepreg material was simulated as homogenous neglecting the reported difference in fibre contents in the skins and the core. In this work two approaches have been used, one that assumes that low viscosity zones exist near the mould surface and one that assumes that the material is homogenous. For the first model different viscosity models are applied in the bulk flow, and in the skins. The thickness of the skins is set constant to 0.25 mm throughout the simulations following the observation in Le et al.[8] that the upper skin had a thickness of 0.22 mm and the lower had a thickness of 0.26 mm for the cured material. A fraction of the constant A, representing the basic viscosity in the bulk flow, is used in the skins. Fibres increase the compression viscosity and it has been shown that the relationship may be described by equation (7). To exemplify fibre fractions of 0.11 and 0.2 increase the compression viscosity by about 25 and 61 times being nearly 10 and more than 20 times more than the increase for the shear viscosity ($f = 0.11$), see the part on rheology in this paper. In this work, it is simply assumed that the addition of fibres increases the shear viscosity by a factor of 3 also for $f = 0.2$. Therefore, A is multiplied by a factor 3/61 in the skins. As mentioned above, studies have indicated that the skin layers are highly sheared and shear-thinning effects have been included in the models by using the shear thinning part of equation (2), which reads

$$\left(1+\dot{\gamma}^2\right)^{\left(\frac{n-1}{2}\right)} \tag{8}$$

In the work by Lee et al.[11] a temperature dependent Newtonian plateau was found for the shear viscosity. A similar Newtonian plateau has been given to models 2 and 4 in this work, presented in Table 3, by using the data presented in Lee et al. [11] and assuming that the material in this work have a similar Newtonian plateau. By adjusting equation (8) to

$$\left(1+\left(8.642960044415\times 10^{15}\times e^{(-0.122629261808*T)}\right)\dot{\gamma}^2\right)^{\left(\frac{n-1}{2}\right)} \tag{9}$$

where it is actually necessarily to keep all figures to get a good fit, the modelled shear thinning acquires a similar Newtonian plateau as in Lee et al.[11] As a consequence, shear-thinning effects become negligible as the SMC temperature increases. For simplicity let the time constant be denoted as

$$\lambda = 8.642960044415\times 10^{15}\times e^{(-0.122629261808\times T)} \tag{10}$$

which now can be seen as a temperature dependant Newtonian constant. For the temperature dependence of the viscosity, an Arrhenius dependence was applied, see equation (1). It was observed in the experiments and previously in the works by Le Corre et al.[12] and Dumont et al.[15] that the compression viscosity had a strain rate dependence, therefore the strain rate part $(\dot{\varepsilon}/\dot{\varepsilon}_0)^{n-1}$ from equations (3) and (4) was included in the models as well. Combining the above equations with the two different approaches in different ways gives a skin approach with a double viscosity model

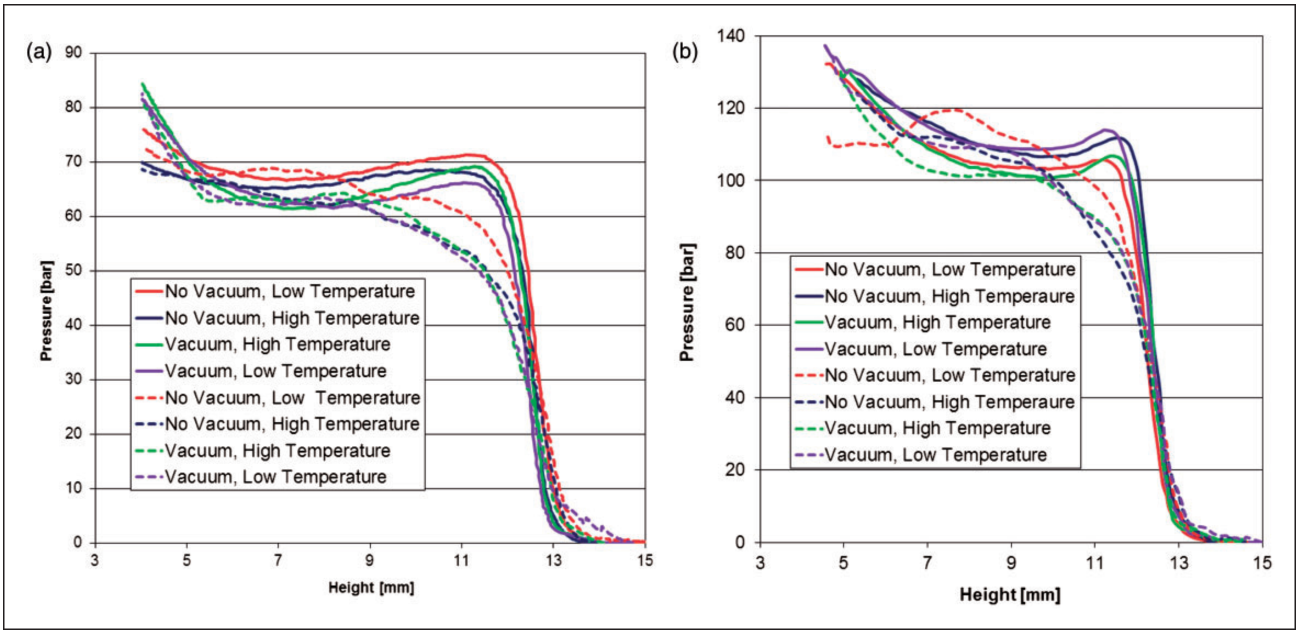

Figure 5. Average pressure for the four replicates at each setting at the low (a) and high (b) mould closing speed. Solid lines show the pressure readings from the centre sensor and dotted lines show the pressure readings from the outer sensor located at the radii 0.07 m.

and a fully bulk approach with one viscosity model which can be seen in Table 3 where the value 0.33 from the experimental results was applied for n.

Results

The experimental and numerical results will be presented here separately. In the first experimental part, the results from the compression moulding experiments will be presented together with the observations made in the additional vacuum test with prepreg at different temperatures. Then the numerical results for the different models will follow.

Experimental results

A summary of the experimental pressure response is presented in Figure 5 where each colour of the curves represents a specific moulding condition for the slow (a) and fast (b) closing velocity and is the average pressure response from four separate mouldings. Solid lines represent pressure readings from the centre sensor while dotted lines represent readings from the outer pressure sensor. From the results it can be seen that the pressure at the centre of the mould rapidly increases until a clear peak forms approximately at the height of 11.4 mm for all conditions tested. The peak is not as distinct for the outer sensor, instead the increase in pressure is flattened out, see the dashed lines in Figure 5. After the first peak for the centre sensor, the pressure then drops a little before it starts to build up again. Interestingly the pressure curves from the outer sensor then border on the ones from the inner sensor indicating that there is a marginal flow and/or a very low viscosity flow. During the period visualised in Figure 5, the press was capable of deforming the sample at constant velocity. However, as the press approached the lowest position, it suddenly decelerated and the pressure quickly decreased and finally reached the applied pressure when the press had reached the lowest position and the SMC had completely filled the cavity. Statistical analysis of the experimental results shows several significant results that were found by using a confidence level of 95%. Here the results are divided into two phases during the closing of the moulding tool. After that the results are interpreted in terms of the compression viscosity.

Phase 1 – Start to the first pressure peak

The height at where the pressure started to increase, meaning the height where the upper mould half reached the SMC charge, was interestingly found to be mainly affected by the level of vacuum even though the samples had approximately the same height from the beginning. On average, the pressure for the samples with applied vacuum started to increase about 0.65 mm above the samples that were moulded without vacuum assistance. The distance of 0.65 mm is short, but it was a significant result. Therefore, an additional simple experiment was carried out where prepreg at different temperatures:

25°C, 50°C and 80°C were placed in a transparent vessel wherein vacuum was applied. For the prepregs at room temperature and 50°C, nothing extraordinary occurred except that the prepregs seemed to dry out after a while. The sample that was preheated to 80°C, however, immediately and rapidly swelled up when the vacuum was applied. A boiling liquid could also be seen at the surface of the transparent vacuum vessel. It is likely that the observed boiling liquid was styrene that had reached its boiling point due to the applied vacuum.[7,20] The simple experiment anyway revealed that the premature increase in pressure on the mould when using vacuum may be a result of a taller charge due to the swelling. Another significant effect during this phase was that the pressure at the first pressure top was mainly affected by the mould closing velocity.

Phase 2 – After the first pressure peak

The distance from the first pressure peak to the position where the minimum pressure occurred was found to be significantly affected by the mould closing velocity. At average, the mould had enclosed 1.9 mm further for the slow than for the fast velocity. The distance between the first pressure top and the height at where the pressure reached the same pressure again was mainly affected by the velocity of the press. At average, the press had moved 2.1 mm further for the low velocity than for the high before it occurred. The closing velocity of the press was set to go at constant velocity the whole way. However, the press did not manage to do this as previously discussed. According to the statistical analysis there where two main effects: velocity and vacuum, and one interaction effect between velocity and temperature that affected the height at where the deceleration was initiated. The largest difference was caused by the velocity setting. At the high velocity, the deceleration occurred earlier than at low velocity. The velocity was also involved in an interaction effect with the temperature level. At slow closing velocity, the press was capable to compress the SMC with constant velocity the same distance for both the high and the low temperature. With the higher closing velocity, the press managed to keep constant velocity further with the higher temperature. Vacuum assistance seemed to aid the press at the end of the moulding phase since the press on average managed to compress the SMC further with constant velocity with applied vacuum assistance. This indicates that vacuum assistance prevents a pressure build-up of entrapped air inside of the moulding tool.

Compression viscosity. Applying equation (5) with the pressure at the pressure peak registered by the centre sensor for the low and high mould closing velocity and with the average result for each process setting it was found that the result followed a power law with the average strain rate sensitivity of $n = 0.33$, ranging from 0.28 to 0.36, see Figure 6. This is slightly lower, and hence less Newtonian, than reported in Dumont et al.[15] (0.44) and Le Corre et al.[12] (0.45). But, following the results that a higher amount of fillers give a less Newtonian behaviour by Boylan et al.,[21] this was expected since the SMC prepreg in this work had a higher amount of filler (66.8% vs. 62%).

The results in the present study are, however, not fully trustworthy since there is a temperature gradient within the charge in this work which probably lowers the compression viscosity more for the low closing velocity than for the high velocity due to longer time in contact with the mould before the pressure top was attained. It is therefore reasonable to assume that if the moulding experiment should be isothermal, the pressure at the low velocity should have been higher in comparison to the pressure at the high closing velocity. As a consequence, n would have approached the expected value 0.3, found from linearization of data presented by Boylan et al.[21] Le Corre et al.[12] applied a constant strain rate and a homogeneous temperature distribution. Here, the velocity was set to constant which gives an increasing strain rate as the mould closes and the gap between the mould halves decreases. From these results, curves could be plotted; see Figure 7 for one example. In the figure it can be seen that the compression viscosity decreases faster in the beginning; this is probably due to preheating from the moulding tool and the squish effect observed by Odenberger et al.[7] At the end, the curve flattens out and n approached the expected value 0.3.

Numerical results

The obtained values of the constants A and B followed by the modelled and experimental pressure for the different models are presented here. Combinations of the constants A and B could be found for each model that resulted in acceptable accurate centre pressure for the slow mould closing velocity. The obtained values can be seen in Table 4. By comparing the models and obtained constants, it can be seen that the values of the constant A are obtained in a rather narrow field. Using equation (7) A can be used to calculate η_0 within the range 62,000–77,000 Pa s. These values are in the same range as the one used in Le Corre et al.,[12] 55,000 Pa s. Depending on the assumptions made, the obtained values of B differ more.

The predicted pressure for each model with the constants in Figure 5 will hereafter be presented, first for the slow ($2.5\,\mathrm{mm\,s^{-1}}$) and then the fast ($10\,\mathrm{mm\,s^{-1}}$) mould closing speed for each model. It was only the

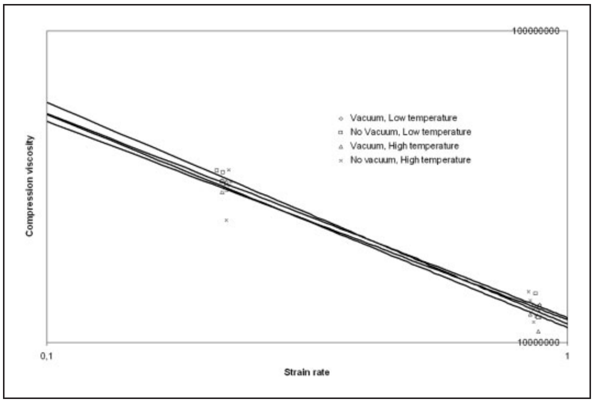

Figure 6. The compression viscosity at the first pressure peak, derived from average values from each setting. The average n is 0.33, and the spread in the result is 0.28–0.36.

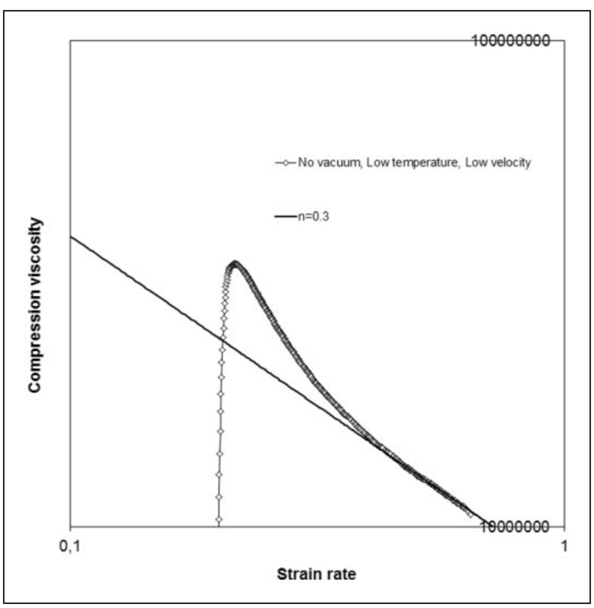

Figure 7. Compression viscosity for a sample from start until the second pressure top seen in Figure 5. The highest value occurs at the logarithmic strain 0.25.

centre pressure that was used when the constants were found, but the outer pressure (at radii 0.07 m) is shown in the results as well with dotted lines. The experimental pressure that is presented together with the numerical results is the average pressure for the mouldings made without vacuum assistance and at the low tool temperature, which is also visible in Figure 5. It was the pressure from these settings in combination with low mould closing velocity that was aimed for when the constants were determined.

Model 1, only bulk, shear thinning. In Figure 8 the modelled pressure for the slow mould closing velocity is shown. As seen, the modelled centre pressure is in very good agreement with experiments. The results for the closing velocity $10\,\mathrm{mm\,s^{-1}}$ using the same constants, but decreasing the preheating time to 0.35 s, are presented in Figure 9. As seen, the centre pressure is in good agreement here as well.

Model 2, only bulk, shear thinning with a Newtonian plateau. This model also neglects the skins, but in addition to the previous model, the shear thinning of this have a temperature dependence and the shear-thinning effect is reduced when the temperature of the material increases. As a consequence, the value of A increased with 17% compared to the previous model while B was increased with 46%. This resulted in good agreement between experiments and numeric for the slow mould closing velocity, see Figure 10. Using the same constants for the high mould closing velocity and shorter preheating time (0.35 s) did however result in a pressure that started to low and then increased to fast, see Figure 11.

Model 3, bulk and skins, both shear thinning. The bulk material is assumed to follow the same model as for the first case presented in Figures 8 and 9, but the material closest to the mould halves is assumed to follow the skin model, see Table 3. Compared to the first model, the constant A is here only increased by 10% while B on the other hand is decreased by 34%. For the slow mould closing velocity, the centre pressure

Table 4. Values that was found to give proper values for the slow closing velocity.

Model		*A*	*B*
1	Only bulk, shear thinning.	11,325,800	6521
2	Only bulk, shear thinning with a Newtonian plateau.	13,280,650	9533.5
3	Bulk and skins, both shear thinning.	12,499,000	4327.5
4	Bulk and skins, both shear thinning with a Newtonian plateau.	14,040,300	7363.5
5	Bulk and skins, only shear thinning in skins.	12,215,900	4685.5

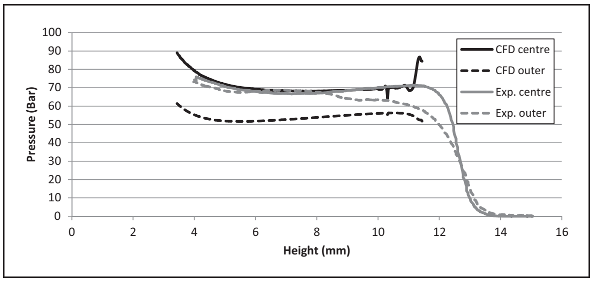

Figure 8. The modelled pressure for 2.5 mm/s with model 1, only bulk, shear thinning.

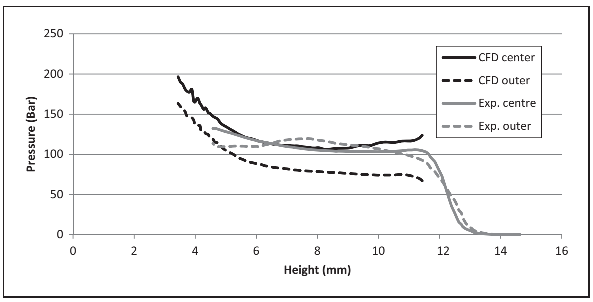

Figure 9. The modelled pressure for 10 mm/s with model 1, only bulk, shear thinning.

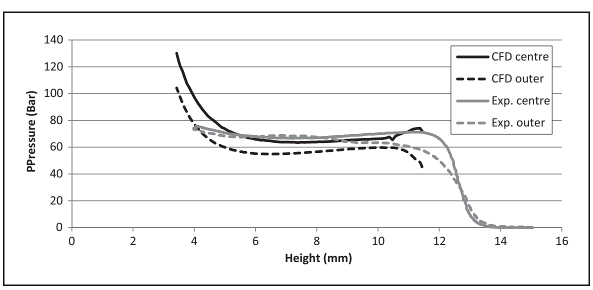

Figure 10. The modelled pressure for 2.5 mm/s with model 2, only bulk, shear thinning with a Newtonian plateau.

is in very good agreement. The outer pressure is also in very good agreement at first, but then there is a deviation at a height of about 9 mm, see Figure 12. In Figure 13 the pressure can be seen when the same constants are used for 10 mm/s and the shorter preheating time (0.35 s). As seen, the numerically and experimentally derived central pressures are in very good agreement here as well.

Model 4, bulk and skins, both shear thinning with a Newtonian plateau. This model is the same as the previous one, except that the shear thinning has the same temperature dependence in the skins and in the bulk as model 2, see Table 3. In order to achieve the desired pressure in the beginning and the end of the pressing, the constant A and B had to be increased by 12% and 70% compared

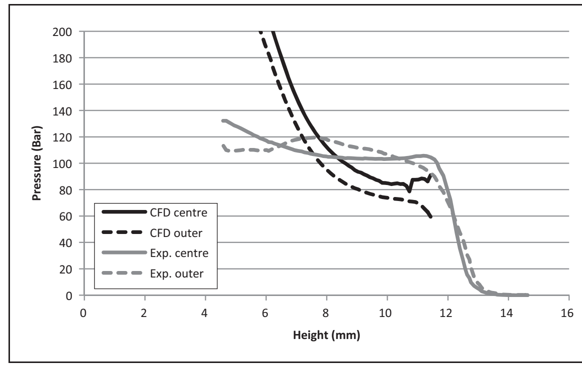

Figure 11. The modelled pressure for 10 mm/s with model 2, only bulk, shear thinning with a Newtonian plateau.

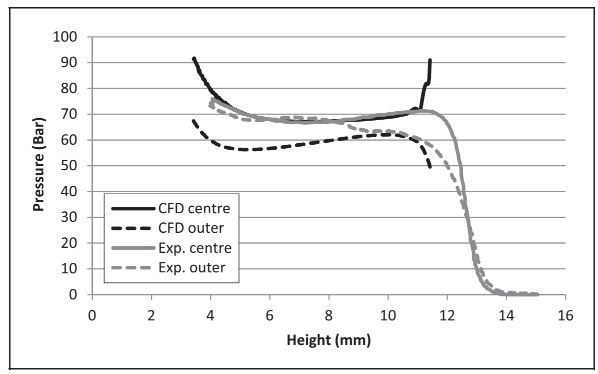

Figure 12. The modelled pressure for 2.5 mm/s with model 3, bulk and skins, both shear thinning.

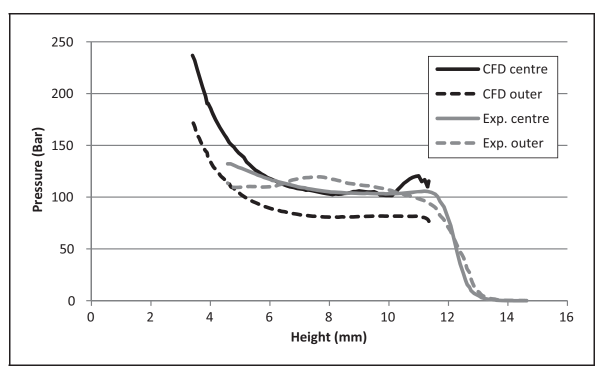

Figure 13. The modelled pressure for 10 mm/s with model 3, bulk and skins, both shear thinning.

to the model, respectively. As seen in Figure 14, these actions resulted in rather good agreement both for the centre and outer pressure. Using the same constants and shorter preheating time for the faster mould closing velocity resulted however in a too high pressure that then has a too step gradient, see Figure 15. In order to investigate how the preheating affected this, an additional simulation was run with a preheating

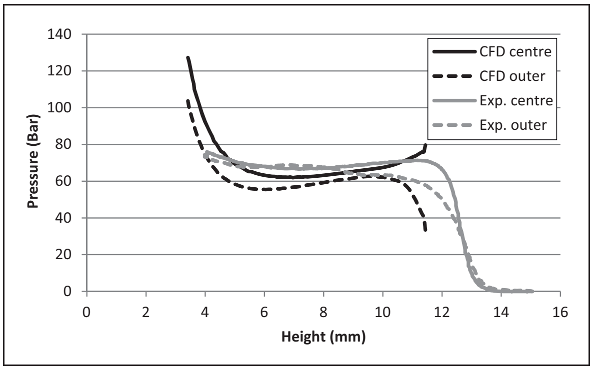

Figure 14. The modelled pressure for 2.5 mm/s with model 4, bulk and skins, both shear thinning with a Newtonian plateau.

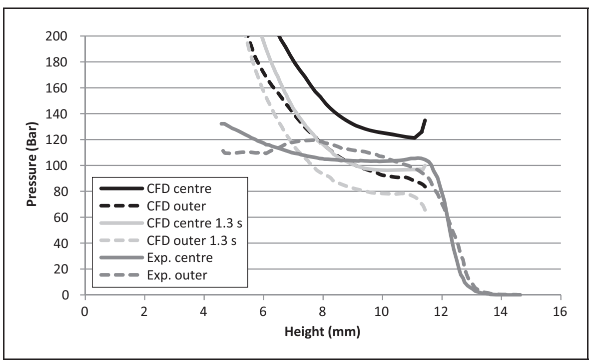

Figure 15. The modelled pressure for 10 mm/s with model 4, bulk and skins, both shear thinning with a Newtonian plateau.

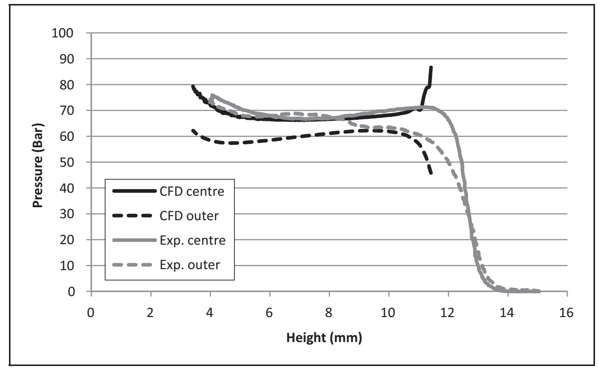

Figure 16. The modelled pressure for 2.5 mm/s with model 5, bulk and skins, only shear thinning in the skins.

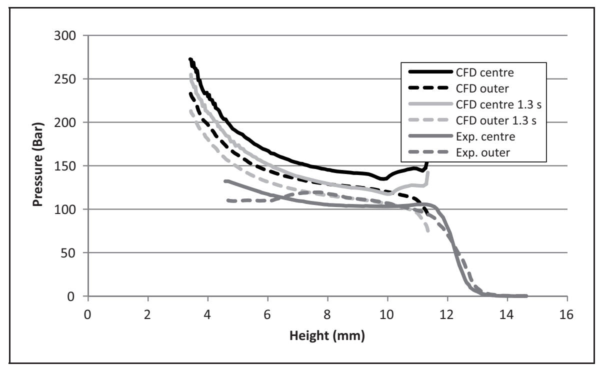

Figure 17. The modelled pressure for 10 mm/s with model 5, bulk and skins, only shear thinning in the skins.

for 1.3 s (the same as in the slow mould closing simulations). This resulted in a more accurate starting pressure, but the pressure then increased to fast with this initial condition as well, this result is also visible in Figure 15.

Model 5, bulk and skins, only shear thinning in the skins. In this model, it is assumed that there exists skin layers that are highly sheared and shear thinning while the bulk viscosity is not affected by shear. Compared to the model with skins and bulk material that also behaves shear thinning, the constant A is decreased only by 2% and B is slightly increased with 8%. For the slow mould closing velocity, this resulted in very good agreement, see Figure 16. For the higher velocity, the modelled pressure however became too high, both with the short (0.35 s) and long (1.3 s) preheating time, see Figure 17.

Discussion

Several viscosity models were tested in this work. All of them could, at least for the centre, predict accurate pressure during moulding at slow mould closing velocity. When the mould closing velocity was increased, it seemed like there was only the models that included shear-thinning effects to the bulk material that could predict accurate pressure. This might indicate that shear-thinning effects have a larger affect than previous anticipated during moulding. The temperature dependence added to the shear thinning in this work was obviously too large since it seemed to decrease almost all shear-thinning effects (where the material was sheared, the temperature was so high that shear thinning did not occur). By adding skins and special viscosity models for them, the viscosity dramatically decreases near the walls. The same behaviour can be accomplished without skins by increasing the temperature dependence constant B. Comparing the pressure for the outer sensor in Figure 5 one can see that there seems to be a higher bump for the outer pressure sensor half way into the moulding for the mouldings without vacuum assistance. It is possible that this occurs due to a pressure build up from encapsulated air. Since the numerical results were compared to these, this is a possible explanation to why the outer pressure did not match as good as the centre pressure. Perhaps it would have been better to compare the numerical results with the experiments made with vacuum assistance.

Conclusions

From this study, it is evident that the viscosity of SMC cannot be described by only the temperature as evaluated in Marjavaara et al. [16] since the viscosity was found to be dependent on the strain rate. However, the approach used by Marjavaara et al.,[16] multiobjective surrogate-based inverse modelling, may very well be useful if a more advanced viscosity model is to be determined from, e.g. model 1, since it turns out that initial conditions and material parameters can be adjusted to get very good fit between simulations and experimental results at different locations in the mould and at different compression speeds. Adjusting the preheating time for the different velocities was necessary to achieve accurate pressure, this is in accordance with the results presented by Shokrieh and Mosalmani.[22] Using the numerical simulations as some sort of viscosity meter, it seems the bulk material of SMC behaves shear thinning. Using the same basic method as in this work, simulation data can easily be set up for various SMC:s in order to run simulations with them without deeper knowledge of their real material properties. The experiments showed that vacuum assistance can aid the press to compress further with constant velocity during compression, possibly by preventing a pressure build-up of encapsulated air inside of the moulding tool. It was furthermore also observed that heated prepreg swelled and that a boiling liquid appeared, probably styrene, when vacuum was applied.

Conflict of interest

None declared.

Funding

This research is supported by the Swedish Agency for Innovation Systems (VINNOVA) and the participating industries in the FYS-project.

References

1. Oldenbo M, Mattsson D, Varna J, et al. Global stiffness of a SMC panel considering process induced fiber orientation. *J Reinf Plast Compos* 2004; 23: 37–49.
2. Sjögren A. An approach towards avoidance of pinholes and blowouts in painted SMC. In: *Internationale AVK-TV*, Tagung Baden, Baden, 2002.
3. Naidu MS and Kamaraju V. *High voltage engineering*, 2nd ed. New York, NY: McGraw-Hill, 1996, p.378.
4. Olsson NEJ, Lundstrom TS and Olofsson K. Design of experiment study of compression moulding of SMC. *Plast Rubber Compos* 2009; 38: 426–431.
5. Comte E, Merhi D, Michaud V, et al. Void formation and transport during SMC manufacturing: effect of the glass fiber sizing. *Polym Compos* 2006; 27: 289–298.
6. Lundstrom TS and Holmgren A. Dissolution of voids during compression moulding of SMC. *J Reinf Plast Compos* 2009; 1826–1837.
7. Odenberger PT, Andersson HM and Lundstrom TS. Experimental flow-front visualisation in compression moulding of SMC. *Compos Part A Appl Sci Manuf* 2004; 35: 1125–1134.
8. Dumont TH, Orgeas PJJ, Le L, et al. X-ray phase contrast microtomography for the analysis of the fibrous microstructure of SMC composites. *Compos Part A Appl Sci Manuf* 2008; 39: 91–103.
9. Yamada H, Mihata I, Tomiyama T, et al. Investigation of the fundamental causes of pinholes in SMC moldings. In: *47th annual conference, composites institute, the society of the plastics industry, Inc*., Cincinnati, Ohio, USA, 1992.
10. Kim DK, Choi HY and Kim N. Experimental investigation and numerical-simulation of Smc in compression molding. *J Mater Process Technol* 1995; 49: 333–344.
11. Lee LJ, Marker LF and Griffith RM. The rheology and mold flow of polyester sheet molding compound. *Polym Compos* 1981; 2: 209–218.
12. Le Corre S, Orgeas L, Favier D, et al. Shear and compression behaviour of sheet moulding compounds. *Compos Sci Technol* 2002; 62: 571–577.
13. Gibson AG and Toll S. Mechanics of the squeeze flow of planar fibre suspensions. *J Non-Newton Fluid Mech* 1999; 82: 1–24.
14. Kia HG. In: Kia HG (ed.) *Sheet molding compounds: Science and technology*. Munich: Hanser, 1993, p.257.
15. Dumont P, Orgeas L, Le Corre S, et al. Anisotropic viscous behavior of sheet molding compounds (SMC) during compression molding. *Int J Plast* 2003; 19: 625–646.
16. Marjavaara BD, Ebermark S and Lundstrom TS. Compression moulding simulations of SMC using a multiobjective surrogate-based inverse modeling approach. *Mech Compos Mater* 2009; 45: 503–514.
17. Rabinovich M, Olsavsky KL, Leach B, et al. Sheet molding compound characterization using spiral flow. *J Appl Polym Sci* 2008; 109: 2465–2471.
18. Dumont P, et al. Compression moulding of SMC: In situ experiments, modelling and simulation. *Composites Part a-Applied Science and Manufacturing* 2007; 38: 353–368.
19. Olofsson K and Sandlund E. *Mätning av Värmeledningstal i SMC 5412. SICOMP CR 08-077*. Institute Swerea SICOMP AB, Piteå, 2008.
20. Lundstrom TS, Gebart BR and Lundemo CY. Void formation in RTM. *J Reinf Plast Compos* 1993; 12: 1339–1349.
21. Boylan S, Abrams LM and Castro JM. Predicting molding forces during sheet molding compound (SMC) compression molding. II: effect of SMC composition. *Polym Compos* 2003; 24: 731–747.

22. Shokrieh MM and Mosalmani R. Modeling of sheet molding compound compression molding under non-isothermal conditions. *J Reinf Plast Compos* 2014; 33: 1183–1198.

Nomenclature

b	temperature constant
f_f	volume fraction of fibres
h	height
n	strain rate sensitivity
T	temperature
$\dot{\gamma}$	shear strain rate
ε	strain
η	viscosity
λ	time constant
σ	stress